



Brain accumulation of tivozanib is restricted by ABCB1 (P-glycoprotein) and ABCG2 (breast cancer resistance protein) in mice

Jing Wang^a, Maaïke A.C. Bruin^{a,b}, Changpei Gan^a, Maria C. Lebre^a, Hilde Rosing^b,
Jos H. Beijnen^{a,b,c}, Alfred H. Schinkel^{a,*}

^a Division of Pharmacology, The Netherlands Cancer Institute, Amsterdam, The Netherlands

^b Department of Pharmacy & Pharmacology, The Netherlands Cancer Institute, Amsterdam, The Netherlands

^c Division of Pharmacoepidemiology and Clinical Pharmacology, Utrecht Institute for Pharmaceutical Sciences, Utrecht University, Utrecht, The Netherlands

ARTICLE INFO

Keywords:

Tivozanib
ABCB1
ABCG2
Oatp1a/1b
CYP3A enzymes
Brain penetration

ABSTRACT

Tivozanib is a potent and selective inhibitor of VEGFR1-3, recently approved by the EMA for first-line treatment of renal cell carcinoma. We used wild-type, knockout, and transgenic mouse strains to study the effects of the drug transporters ABCB1, ABCG2, and OATP1A/1B, and of the CYP3A enzymes on the oral availability and tissue distribution of tivozanib. Tivozanib was transported by human ABCB1 and mouse Abcg2 in polarized MDCK-II cells. Upon oral administration, tivozanib showed rapid absorption and the plasma concentration-time curves showed secondary peaks in all mouse strains, suggesting enterohepatic recirculation. The brain-to-plasma ratios were significantly increased in *Abcb1a/1b*^{-/-} (2.2-fold) and *Abcb1a/1b;Abcg2*^{-/-} (2.6-fold) mice compared to wild-type mice, indicating a modest protective role of these transporters in the blood-brain barrier. *Slco1a/1b*^{-/-} mice showed a 1.2-fold lower liver-to-plasma ratio than wild-type mice, suggesting a minor role of mOatp1a/1b in tivozanib liver distribution. Oral plasma pharmacokinetics of tivozanib was not significantly altered in these mouse strains, nor in Cyp3a knockout and CYP3A4-humanized mice. The modest effect of ABC transporters on tivozanib brain accumulation, if also true in humans, might mean that this drug is not strongly limited in its therapeutic efficacy against malignant lesions situated partly or completely behind the blood-brain barrier.

1. Introduction

Renal cell carcinoma (RCC) is the most common type of kidney cancer, originating in the lining of the renal proximal convoluted tubule. It accounts for 90–95% of neoplasms arising from the kidney and for 2% to 3% of all adult malignancies (EMA 2017). In RCC, overexpression of vascular endothelial growth factor (VEGF) and platelet-derived growth factor promotes neoangiogenesis, which contributes to the development and progression of RCC. About 25–30% of patients have metastatic disease at diagnosis, the most common sites being lung (45%), bone (30%), lymph nodes (22%), liver (20%), adrenal (9%) and brain (9%) (Bianchi et al. 2011, Gong et al. 2016).

Tivozanib (Fotivda, AV-951, Supplemental Fig. 1) is an oral, once-daily administered, VEGF receptor tyrosine kinase inhibitor (TKI). This hydrophobic drug (logP = 4) has a long half-life and is a potent and selective inhibitor of all three VEGF receptors (VEGFR1-3), inhibiting angiogenesis and reducing the vascular permeability in tumor tissues. Tivozanib has been investigated in several tumor types, including renal

cell, hepatocellular, colorectal and breast cancers. In August 2017, tivozanib was approved by the European Medicines Agency (EMA) for the first-line treatment of adult patients with advanced RCC and for adult patients who are VEGFR and mTOR pathway inhibitor-naïve following disease progression after one prior treatment with cytokine therapy for advanced RCC (AVEO Oncology 2017). One Phase III study showed that tivozanib was generally well tolerated, and significantly improved progression-free survival (PFS) compared with sorafenib (VEGFR inhibitor) in patients with metastatic RCC (Motzer et al. 2013).

Transmembrane transporters can be major determinants of the pharmacokinetic, safety and efficacy profiles of drugs (Giacomini et al. 2010). P-glycoprotein (P-gp; ABCB1) and breast cancer resistance protein (BCRP; ABCG2), multispecific efflux transporters of the ATP-binding cassette (ABC) superfamily, are localized in the canalicular membranes of hepatocytes and in the apical membrane of epithelial cells of the intestinal tract and kidney. They can therefore potentially limit intestinal absorption of their substrates or mediate their direct intestinal, hepatobiliary, or renal excretion. ABCB1 and ABCG2 are also

* Corresponding author at: The Netherlands Cancer Institute, Division of Pharmacology, Plesmanlaan 121, 1066 CX Amsterdam, The Netherlands.

E-mail address: a.schinkel@nki.nl (A.H. Schinkel).

<https://doi.org/10.1016/j.ijpharm.2020.119277>

Received 7 January 2020; Received in revised form 18 March 2020; Accepted 25 March 2020

Available online 28 March 2020

0378-5173/© 2020 Elsevier B.V. All rights reserved.

present at the blood–brain barrier (BBB), where they can pump their substrates back into the blood (Borst and Elferink 2002, Schinkel and Jonker 2003, Vlaming et al. 2009). Limited exposure of the brain to anticancer drugs due to these transporters may reduce their therapeutic efficacy, especially against brain metastases (Wang et al. 2018, Wang et al. 2019). There is contradictory information in the literature on the interaction between tivozanib and ABCB1 and ABCG2. Yang et al. (2014) found that tivozanib is a modest inhibitor of human (h)ABCB1 and hABCG2 *in vitro*, and that tivozanib could slightly stimulate their ATPase activity. In contrast, the EMA registration information (EMA 2017) stated that tivozanib is neither a substrate nor an inhibitor of hABCB1, although it could inhibit hABCG2 *in vitro*. The EMA suggested the need for further investigation of tivozanib as a transport substrate for hABCB1 and hABCG2 as a post-authorization measure.

Organic anion transporting polypeptides (human: OATP, gene *SLCO*; rodents: Oatp, gene *Slco*) are primarily uptake transporters for drugs and endogenous compounds. The OATP1A and 1B subfamilies are expressed in pharmacokinetically relevant tissues like liver, kidney and small intestine in both human and mice, where they can be important in the absorption, distribution and elimination of many drugs including anticancer drugs (Cheng et al. 2005, Cheng and Klaassen 2009, van de Steeg et al. 2010). Little is known on whether tivozanib can be transported by the OATP1A/1B transporters.

Cytochrome P450-3A (CYP3A) is the most abundant human CYP subfamily, and highly expressed in liver and small intestine. It therefore plays a significant role in the oxidative metabolism of approximately half of the drugs in current clinical use (Guengerich 1995, Zanger and Schwab 2013). As CYP3A activity can display a high degree of inter- and intra-individual variation, it is a major player in variable drug exposure (van Waterschoot et al. 2009, van Hoppe et al. 2017). *In vitro* tivozanib is modestly metabolized by CYP3A4 and CYP1A1, and although a clinical study showed no significant impact of CYP3A inhibition on tivozanib plasma levels, the CYP3A-inducing drug rifampin did result in decreased plasma levels (Cotreau et al. 2015). This raises the question whether tivozanib can be substantially impacted by CYP3A activity *in vivo*.

In view of these uncertainties, we here aimed to investigate whether tivozanib is transported by ABCB1 and ABCG2, and to establish the individual and combined effects of the ABCB1, ABCG2, and OATP1A/1B drug transporters on the oral availability and tissue distribution of tivozanib using wild-type and transporter knockout mouse strains. We also studied to what extent mouse and human CYP3A can affect the oral availability of tivozanib using Cyp3a knockout mice and transgenic mice.

2. Material and methods

2.1. Chemicals

Tivozanib free base (> 99%, $M_w = 454.9$ g/mol, Supplemental Fig. 1) was obtained from Carbosynth (Compton, Berkshire, UK). Zosuquidar was obtained from Sequoia Research Products (Pangbourne, UK), and Ko143 was from Tocris Bioscience (Bristol, UK). Bovine Serum Albumin (BSA) Fraction V was obtained from Roche Diagnostics (Mannheim, Germany). Heparin (5000 IU ml^{-1}) was from Leo Pharma (Breda, The Netherlands), isoflurane was purchased from Pharmachemie (Haarlem, The Netherlands). Bovine Serum Albumin (BSA) Fraction V from Roche (Mannheim, Germany). All other chemicals and reagents were obtained from Sigma-Aldrich (Steinheim, Germany). All chemicals used in the tivozanib assay were described before (Bruin et al. 2019).

2.2. Transport assays

Polarized Madin-Darby Canine Kidney (MDCK-II) cell lines transfected with either human (h)ABCB1, hABCG2 or mouse (m)Abcg2

cDNA were used (passage 10–20 after clonal selection) and cultured as described previously (Durmus et al. 2012). Transport proficiency of these cell lines is continually monitored by testing transport of various other tyrosine kinase inhibitor drugs (e.g., larotrectinib, DOI: <https://doi.org/10.1111/bph.15034>). Transepithelial transport assays were performed on microporous polycarbonate membrane filters (3.0 mm pore size, 12 mm diameter, Transwell 3402, Corning Incorporated, Kennebunk, ME). In short, cells were allowed to grow an intact monolayer in 3 days, which was monitored with transepithelial electrical resistance (TEER) measurements, both before and after the transport phase. TEER values had to be at or above 80 Ohm.cm², which is typical for these cell lines. On the third day, if applicable, cells were pre-incubated with one or more of the inhibitors for 1 h, where 5 μM zosuquidar (ABCB1 inhibitor) and/or 5 μM Ko143 (ABCG2/Abcg2 inhibitor) were added to both apical and basolateral compartments. The transport phase was initiated ($t = 0$) by replacing the medium in both compartments with fresh Dulbecco's Modified Eagle's medium (DMEM medium) including 10% fetal bovine serum (FBS) and 2 μM tivozanib, as well as the appropriate inhibitor(s). Cells were kept at 37 °C in 5% (v/v) CO₂ during the experiment, and at 1, 2, 4 and 8 h, 50 μl samples were taken from the acceptor compartment, and stored at –30 °C until LC-MS/MS analysis. Before each sampling, plates were gently rocked to ensure homogeneity of the well contents. The amount of transported drug was calculated after correction for volume loss due to sampling at each time point. Active transport was expressed using the transport ratio (r), which is defined as the amount of apically directed drug transport divided by basolaterally directed drug translocation at 8 h.

2.3. Animals

Mice (*Mus musculus*) were bred in the Netherlands Cancer Institute and housed and handled according to institutional guidelines complying with Dutch and EU legislation. Animals used were female WT, *Abcb1a/1b*^{−/−} (Schinkel et al. 1997), *Abcg2*^{−/−} (Jonker et al. 2002), *Abcb1a/1b;Abcg2*^{−/−} (Jonker et al. 2005), *Cyp3a*^{−/−} (van Herwaarden et al. 2007) and *Slco1a/1b*^{−/−} (van de Steeg et al. 2010) mice of a > 99% FVB/N strain background. Homozygous CYP3A4 humanized transgenic mice (Cyp3aXAV) were generated by cross-breeding of transgenic mice with stable human CYP3A4 expression in liver or intestine, respectively, in a *Cyp3a*^{−/−} background (van Herwaarden et al. 2007). All the mice used were between 9 and 14 weeks of age, and generally between 23 and 35 g of body weight. Animals were kept in a temperature-controlled environment with a 12 h light/12 h dark cycle and received a standard diet (Transbreed, SDS Diets, Technilab-BMI) and acidified water *ad libitum*. Depending on the type of experiment, between 4 and 6 mice were tested in each experimental group. All experiments were reviewed and approved by the Institutional Animal Care and Use Committee (IACUC).

2.4. Drug solutions

Tivozanib stock solution in dimethyl sulfoxide (DMSO) at a concentration of 5 mg/ml was stored at –30 °C, and additionally 2:3 (v/v) diluted with a mixture of polysorbate 80/ethanol (1:1, v/v). It was then further diluted with 5% (w/v) glucose in water to yield a working concentration of 0.1 mg/ml. The final tivozanib solution in water contains 2% DMSO, 1.5% (v/v) polysorbate 80, 1.5% (v/v) ethanol, and 4.75% (w/v) glucose. All working solutions were freshly prepared on the day of the experiment.

2.5. Plasma and tissue pharmacokinetics of tivozanib

To minimize variation in absorption, mice were fasted for about 3 h before tivozanib was administered by gavage into the stomach ($n = 5–7$), using a blunt-ended needle. For the 24 or 8 h experiments, 50 μl blood samples were collected from the tail vein at 5 min, 30 min,

1, 2, 4 and 8 h or 5 min, 30 min, 1, 2 and 4 h, respectively, using heparin-coated capillaries (Sarstedt, Germany). At 24 or 8 h, mice were anesthetized with isoflurane and blood was collected by cardiac puncture. The mice were then sacrificed by cervical dislocation, and the brain and a set of other tissues were rapidly removed, weighed and rapidly frozen at -30°C . Organs were homogenized on ice in appropriate volumes of 4% (w/v) BSA in water using a FastPrep®-24 device (MP Biomedicals, SA, California, USA), and then stored at -30°C until analysis. Blood samples were centrifuged at 9,000 g for 6 min at 4°C immediately after collection, and plasma was collected and stored at -30°C until analysis.

2.6. LC-MS/MS analysis

Tivozanib concentrations in cell culture medium, plasma and tissue homogenates were analyzed with a previously reported liquid-chromatography tandem mass spectrometric (LC-MS/MS) assay, using a deuterated internal standard (Bruin et al. 2019).

2.7. Pharmacokinetic and statistics calculations

Pharmacokinetic parameters were calculated by the software GraphPad Prism7 (GraphPad Software Inc., La Jolla, CA, USA). Ordinary one-way analysis of variance (ANOVA) was used to determine significance of differences between groups, after which post-hoc tests with Tukey correction were performed for comparison between individual groups. The two-sided unpaired Student's *t* test was used when treatments or differences between two groups were compared. The area under the plasma concentration–time curve (AUC) was calculated using the trapezoidal rule with the Microsoft Excel plug in PKsolver (Zhang et al. 2010), without extrapolating to infinity. The peak plasma concentration (C_{max}) and the time to reach C_{max} (t_{max}) were estimated from the original data. Differences were considered statistically significant when $P < 0.05$. Data are presented as mean \pm SD with each experimental group containing 5–7 mice.

3. Results

3.1. Tivozanib is moderately transported by hABCB1 and mAbcg2 in vitro

We analyzed tivozanib (2 μM) transport across polarized monolayers of Madin-Darby Canine Kidney (MDCK-II) cell lines stably transduced with hABCB1, hABCG2 or mAbcg2 cDNAs. The parental MDCK-II cell line did not show apically directed transport (Fig. 1A, $r = 0.8$) and addition of the potent ABCB1 inhibitor zosuquidar did not change this result (Fig. 1B, $r = 0.9$). This indicates that endogenously present canine ABCB1 did not noticeably transport tivozanib in the parental cells. In the hABCB1 overexpressing cells, we observed modest apically directed transport of tivozanib (Fig. 1C, $r = 1.8$), which was effectively inhibited by addition of zosuquidar (Fig. 1D, $r = 1.1$). To evaluate the interaction between ABCG2 and tivozanib, zosuquidar was added to inhibit any endogenous canine ABCB1 in experiments with MDCK-II cells overexpressing hABCG2 and mAbcg2. In the hABCG2 subclone we did not detect active transport of tivozanib and addition of Ko143 did not alter this profile (respective $r = 1.0$ and 0.8 , Fig. 1E and F). However, mAbcg2 modestly transported tivozanib in the apical direction (Fig. 1G, $r = 1.8$), and this transport was completely abrogated by treatment with the ABCG2 inhibitor Ko143 (Fig. 1H, $r = 1.0$). Overall, tivozanib appears to be modestly transported by hABCB1 and mAbcg2 in vitro.

3.2. Brain accumulation of tivozanib is limited by mAbcb1 and mAbcg2 activity after oral administration

Tivozanib is orally administered to patients at a dose of 1.5 mg/d. To allow sensitive detection in tissues, mice received tivozanib by oral

gavage into the stomach at a relatively higher dose of 1 mg/kg, yielding maximal plasma levels that were about 5-fold higher than steady state levels in chronically treated patients. We first performed a pilot study using female wild-type (WT) and combination mAbcb1a/1b and mAbcg2 knockout mice, analyzing tivozanib oral availability and tissue disposition over 24 h. As shown in Fig. 2A and Table 1, oral absorption of tivozanib was rapid, with the highest concentrations observed 30 min after dosing. The plasma concentration–time curves showed secondary plasma peaks in individual mice, resulting in plateau-like exposure levels between 0.5 and 8 h. The plasma AUC_{0–24h} revealed no significant differences in tivozanib oral availability between WT and Abcb1a/1b;Abcg2^{-/-} mice. Moreover, the semi-log plot of the plasma concentrations showed similar elimination rates of tivozanib between 8 and 24 h in these two mouse strains (Supplemental Fig. 2A).

We also measured the impact of the ABC transporters on the brain concentration of tivozanib at 24 h. Although plasma AUC over 24 h showed no significant differences between WT and Abcb1a/1b;Abcg2^{-/-} mice, the brain concentration was 4.1-fold increased in the Abcb1a/1b;Abcg2^{-/-} mice compared to WT mice, and 2.1-fold increased when considering the brain-to-plasma ratio (Fig. 3A, B; Table 1). Next, we analyzed liver, kidney, spleen, and small intestinal tissue (SI) concentrations of tivozanib at 24 h. We found no meaningful differences in tissue concentrations or tissue-to-plasma ratios between WT and Abcb1a/1b;Abcg2^{-/-} mice (Supplemental Figs. 3 and 4A, B). Tissue to plasma distribution ratios were about 200%, 150%, 60% and 150% for liver, kidney, spleen, and SI, respectively, which was far higher than observed for the brain (17%) in WT mice. When the percentage of dose of tivozanib retrieved from the small intestinal contents (SIC%) was measured, it was low in both strains, about 0.03% at this time point (Supplemental Fig. 4C).

3.3. CYP3A has little impact on tivozanib plasma pharmacokinetics and tissue disposition 24 h after oral administration

To investigate the impact of CYP3A-mediated metabolism on tivozanib kinetics, we performed a 24 h pilot study using Cyp3a^{-/-}, and mice with specific transgenic overexpression of human CYP3A4 in liver and intestine in a Cyp3a^{-/-} background (Cyp3aXAV mice). After oral administration, tivozanib was rapidly absorbed in all strains, with a t_{max} at or before 30 min, and the plasma curve again showed secondary peaks in all strains (Fig. 2B). Plasma exposure of tivozanib over 24 h (AUC_{0–24}) was not significantly different between the strains, but the semi-log plot of the plasma concentrations suggested a slower elimination rate between 8 and 24 h in Cyp3a^{-/-} and Cyp3aXAV mice compared to WT mice (Supplemental Fig. 2B).

After oral administration, Cyp3a^{-/-} and Cyp3aXAV mice showed 2.5-fold and 4.7-fold higher brain concentration than WT mice at 24 h. However, these differences likely reflect the differences in plasma tivozanib concentration at this time point, as suggested by the absence of differences in brain-to-plasma ratios between the strains (Fig. 3A, B; Table 1). The same applied for tivozanib distribution to the liver, kidney, spleen, SI and SIC% of these mouse strains when considering the tissue-to-plasma ratios, except for a borderline difference observed for spleen in Cyp3aXAV mice (Supplemental Figs. 3 and 4). The total amount of tivozanib retrieved from small intestinal content was again low in all strains (Supplemental Fig. 4C).

3.4. Brain accumulation of tivozanib is limited by mAbcb1 and mAbcg2 activity after oral administration at 8 h

Upon oral administration of tivozanib, we observed secondary plasma peaks at ~ 8 h in WT and Abcb1a/1b;Abcg2^{-/-} mice (Fig. 2A). Therefore we performed an 8 h pilot study with oral tivozanib at 1 mg/kg in female WT and Abcb1a/1b;Abcg2^{-/-} mice to assess tissue distribution when the plasma concentration was still high.

As shown in Supplemental Figure 5A, tivozanib showed an average

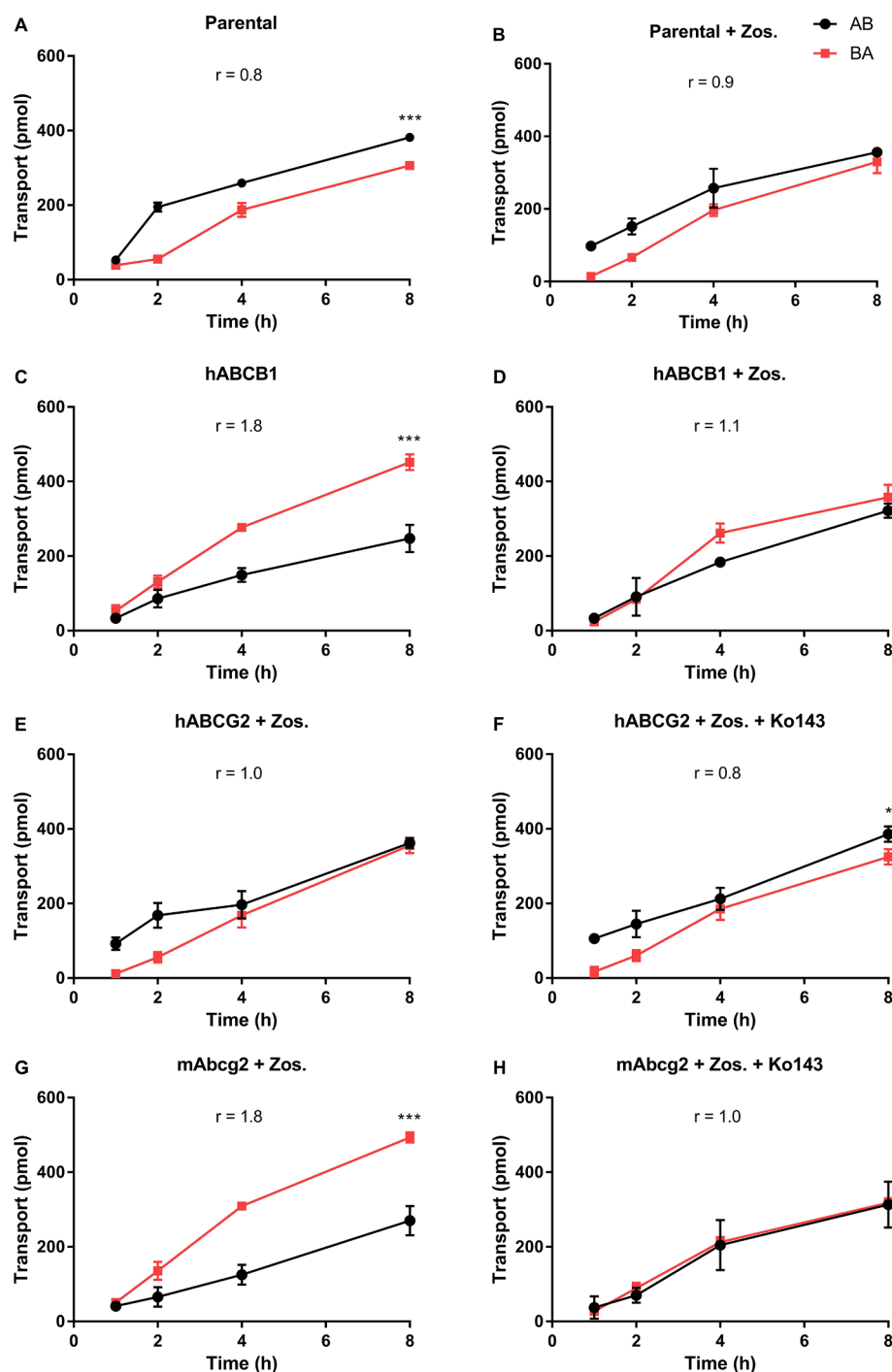


Fig. 1. Transepithelial transport of tivozanib (2 μ M) assessed in MDCK-II cells either non-transduced (A, B), or transduced with hABCB1 (C, D), hABCG2 (E, F) or mAbcg2 (G, H) cDNA. At $t = 0$ h, tivozanib was applied in the donor compartment and the concentrations in the acceptor compartment at $t = 1, 2, 4$ and 8 h were measured and plotted as tivozanib transport (pmol) in the graph ($n = 3$). B, D–H: Zos. (zosuquidar, 5 μ M) was applied to inhibit endogenous and/or human canine ABCB1. F and H: the ABCG2 inhibitor Ko143 (5 μ M) was applied to inhibit ABCG2/Abcg2-mediated transport. r , relative transport ratio at 8 h. BA (■), translocation from the basolateral to the apical compartment; AB (●), translocation from the apical to the basolateral compartment. Data are given as mean \pm S.D. ($n = 3$). *, $P < 0.05$; **, $P < 0.01$; ***, $P < 0.001$ comparing BA to AB at 8 h.

plasma t_{max} at the first time point, 15 min, and the plasma AUC_{0-8h} showed no significant differences. However, at 8 h we observed significant increases in brain concentration (3.3-fold) and brain-to-plasma ratio (2.5-fold) in *Abcb1a/1b;Abcg2*^{-/-} mice in comparison to WT mice (Supplemental Figure 6A, B; Supplemental Table 1). In contrast to the brain-to-plasma ratio, we found a 1.4-fold decreased liver-to-plasma ratio in *Abcb1a/1b;Abcg2*^{-/-} mice compared to WT mice ($P < 0.001$, Supplemental Figure 6D; Supplemental Table 1). We next measured kidney, spleen, lung, SI and SIC% concentrations of tivozanib at 8 h after oral administration (Supplemental Figures 6 and 7; Supplemental Table 1). The tissue-to-plasma ratios showed no statistically significant differences between WT and *Abcb1a/1b;Abcg2*^{-/-} mice.

3.5. CYP3A has little impact on tivozanib plasma pharmacokinetics and tissue disposition 8 h after oral administration

A similar pilot experiment over 8 h was performed in WT, *Cyp3a*^{-/-} and *Cyp3aXAV* mice. After oral administration, the highest plasma levels occurred at 15 min, and the plasma AUC_{0-8h} showed no significant differences between these three mouse strains (Fig. 2D). The tivozanib tissue distribution in the major organs tested (brain, liver, kidney, spleen, lung, SI and SIC%) showed no meaningful differences (Supplemental Figures 6 and 7), in line with the 24 h experiment. This suggests that Cyp3a does not have a marked impact on the tissue concentrations of tivozanib after oral administration.

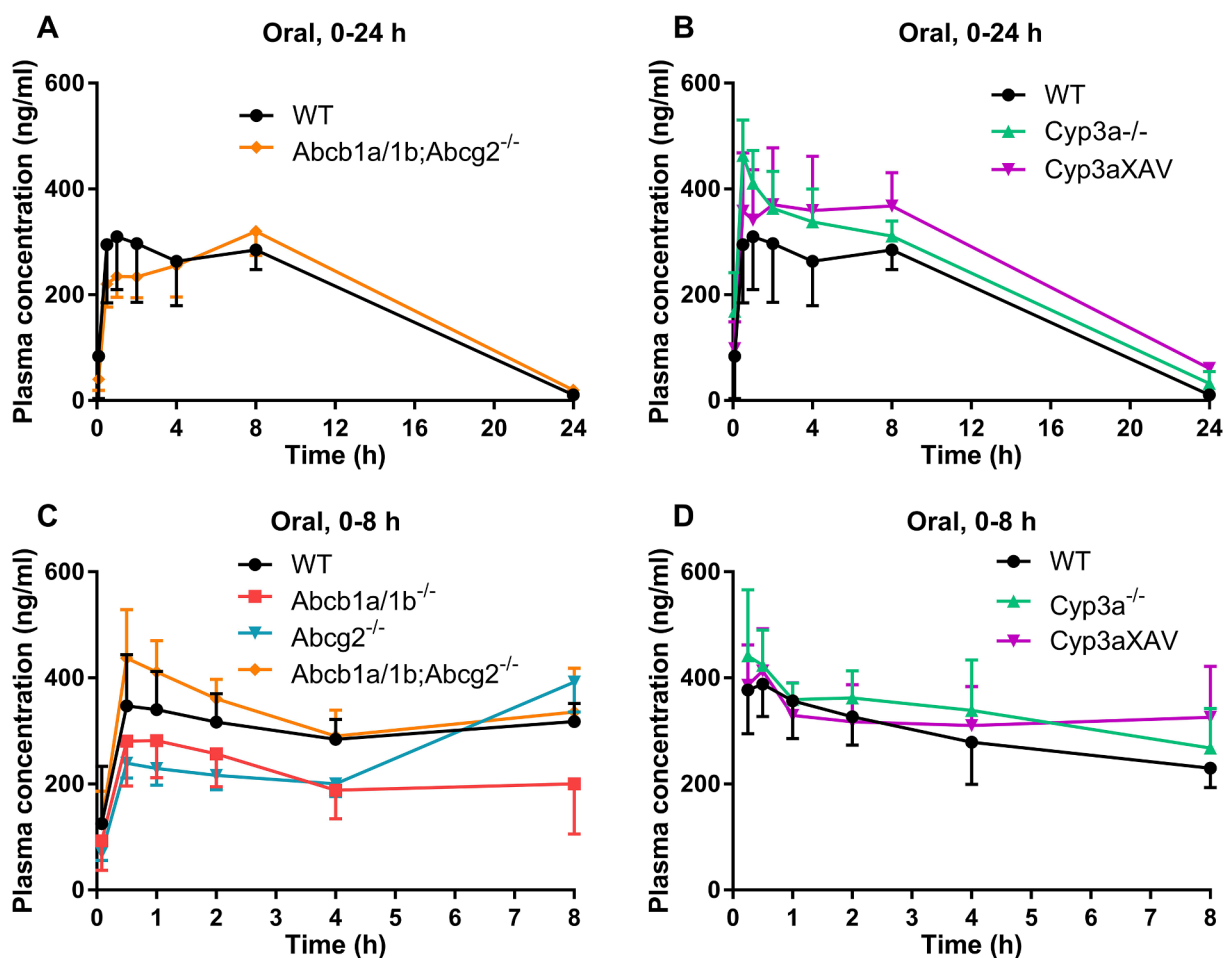


Fig. 2. Plasma concentration–time curves of tivozanib in female mice after oral administration of 1 mg/kg tivozanib. Data are given as mean \pm S.D. (n = 5–7). A: 0–24 h experiment in WT and *Abcb1a/1b;Abcg2*^{-/-} mice. B: 0–24 h experiment in WT, *Cyp3a*^{-/-}, and *Cyp3aXAV* mice. C: 0–8 h experiment in WT, *Abcb1a/1b*^{-/-}, *Abcg2*^{-/-} and *Abcb1a/1b;Abcg2*^{-/-} mice. D: 0–8 h experiment in WT, *Cyp3a*^{-/-}, and *Cyp3aXAV* mice.

3.6. Brain accumulation of tivozanib is limited by both *mAbcb1* and *mAbcg2* after oral administration over 8 h

Upon oral administration of tivozanib and analysis over 24 h and

8 h, the brain penetration of tivozanib was enhanced by combined deficiency of *mAbcb1a/1b* and *mAbcg2*. We therefore performed an 8 h main experiment in WT and *Abcb1a/1b;Abcg2*^{-/-} mice, as well as in separate *Abcb1a/1b* and *Abcg2* knockout strains to look at possible

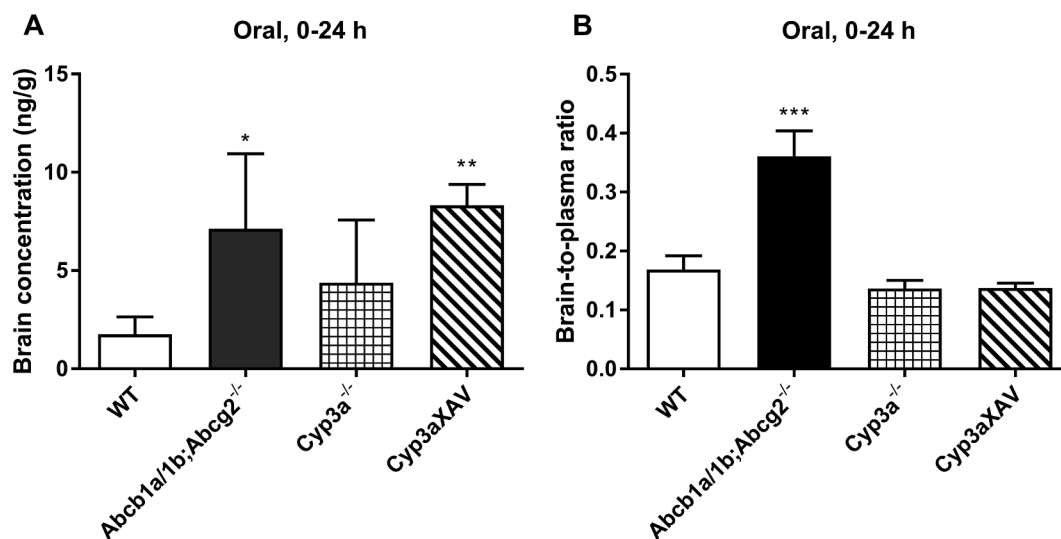


Fig. 3. Brain concentration (A) and brain-to-plasma ratio (B) of tivozanib in female WT, *Abcb1a/1b;Abcg2*^{-/-}, *Cyp3a*^{-/-} and *Cyp3aXAV* mice 24 h after oral administration of 1 mg/kg tivozanib. Data are given as mean \pm S.D. (n = 5–7). *, $P < 0.05$; **, $P < 0.01$; ***, $P < 0.001$ compared to WT mice.

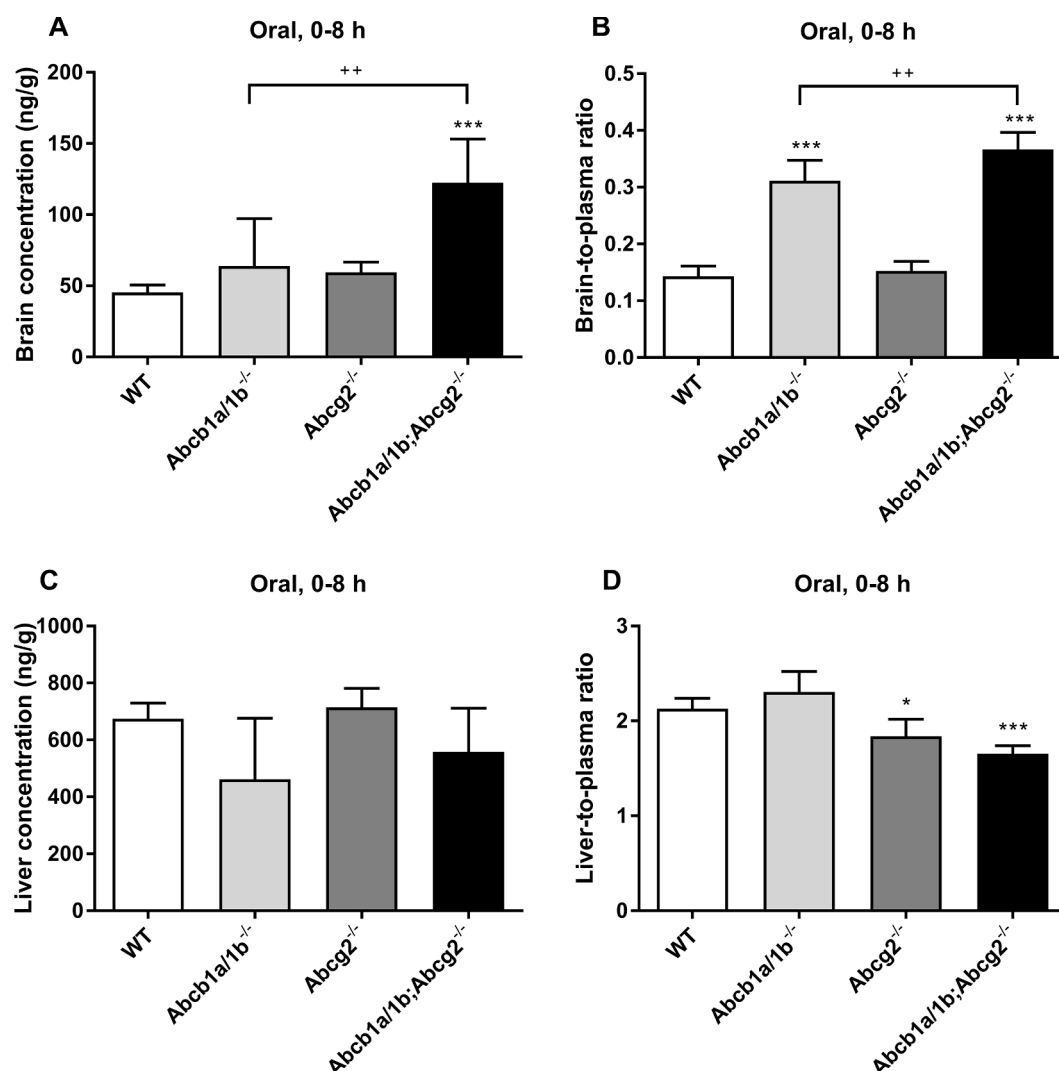


Fig. 4. Brain and liver concentrations (A, C) and brain- and liver-to-plasma ratios (B, D) of tivozanib in female WT, *Abcb1a/1b*^{-/-}, *Abcg2*^{-/-}, and *Abcb1a/1b;Abcg2*^{-/-} mice 8 h after oral administration of 1 mg/kg tivozanib. Data are given as mean \pm S.D. (n = 5–7). *, $P < 0.05$; **, $P < 0.01$; ***, $P < 0.001$ compared to WT mice. ++, $P < 0.01$ comparing *Abcb1a/1b*^{-/-} and *Abcb1a/1b;Abcg2*^{-/-} mice.

Table 1

Plasma pharmacokinetic parameters and tissue concentrations over 24 h after oral administration of 1 mg/kg tivozanib to female WT, *Abcb1a/1b;Abcg2*^{-/-}, *Cyp3a*^{-/-} and *Cyp3aXAV* mice.

Parameter	Genotype			
	WT	<i>Abcb1a/1b;Abcg2</i> ^{-/-}	<i>Cyp3a</i> ^{-/-}	<i>Cyp3aXAV</i>
Plasma AUC _{0-24h} (h*ng/ml)	4557 \pm 683	4756 \pm 674	5481 \pm 179	6227 \pm 936
Fold change AUC _{0-24h}	1.0	1.04	1.20	1.37
C _{max} (ng/ml)	341 \pm 76	322 \pm 46	463 \pm 67	417 \pm 58
t _{max} (h)	0.5–8	4–8	0.5	0.5–8
C _{brain} (ng/g)	1.76 \pm 0.88	7.13 \pm 3.82*	4.38 \pm 3.19	8.32 \pm 1.05***
Fold change C _{brain}	1.0	4.1	2.5	4.7
Brain-to-plasma ratio	0.17 \pm 0.02	0.36 \pm 0.04***	0.14 \pm 0.01	0.14 \pm 0.01
Fold change ratio	1.0	2.1	0.8	0.8

Data are given as mean \pm S.D. (n = 5–7). C_{brain}, brain concentration. *, $P < 0.05$; **, $P < 0.01$; ***, $P < 0.001$ compared to WT mice.

single and overlapping pharmacokinetic roles of these transporters. Since in the previous 8 h pilot experiment we observed t_{max} at the first time point (15 min) after dosing, in this main experiment the first plasma sample was collected at 5 min after dosing.

As before, no significant differences were observed in the oral plasma AUC₀₋₈ in all the mouse strains, even though there was a tendency for the AUC₀₋₈ to be lower in the single *Abcb1a/1b* knockout

mice (Fig. 2C; Table 2). Plasma concentration–time curves showed secondary peaks in all strains (Fig. 2C). We also measured brain, liver, kidney and spleen concentrations of tivozanib at 8 h. The single *Abcg2*^{-/-} mice did not display statistically significant changes in brain concentrations or brain-to-plasma ratios compared to WT mice. However, in spite of the different plasma concentrations at 8 h, the tivozanib brain concentrations were increased about 2.7-fold in *Abcb1a/*

Table 2

Plasma pharmacokinetic parameters and tissue concentrations over 8 h after oral administration of 1 mg/kg tivozanib to female WT, *Abcb1a/1b*^{-/-}, *Abcg2*^{-/-}, and *Abcb1a/1b;Abcg2*^{-/-} mice.

Parameter	Genotype			
	WT	<i>Abcb1a/1b</i> ^{-/-}	<i>Abcg2</i> ^{-/-}	<i>Abcb1a/1b;Abcg2</i> ^{-/-}
Plasma AUC _{0-8h} (h*ng/ml)	2408 ± 229	1713 ± 511	2008 ± 228	2623 ± 322
Fold change AUC _{0-8h}	1.0	0.71	0.83	1.09
C _{max} (ng/ml)	376 ± 82	293 ± 80	392 ± 56	450 ± 80
t _{max} (h)	0.5–8	0.5–8	8	0.5–8
C _{brain} (ng/g)	45.3 ± 5.4	63.8 ± 33.3 ⁺⁺	59.4 ± 7.2	122 ± 31 ^{***}
Fold change C _{brain}	1.0	1.41	1.31	2.70
Brain-to-plasma ratio	0.14 ± 0.02	0.31 ± 0.04 ⁺⁺	0.15 ± 0.02	0.37 ± 0.03 ^{***}
Fold change ratio	1.0	2.2	1.1	2.6
C _{liver} (ng/g)	675 ± 55	462 ± 215	715 ± 67	558 ± 153
Fold change C _{liver}	1.0	0.7	1.1	0.8
Liver-to-plasma ratio	2.13 ± 0.11	2.31 ± 0.22	1.84 ± 0.18	1.65 ± 0.09 ^{***}
Fold change ratio	1.0	1.1	0.9	0.8

Data are given as mean ± S.D. (n = 5–7). C_{tissue}, tissue concentration. *, *P* < 0.05; **, *P* < 0.01; ***, *P* < 0.001 compared to WT mice. ++, *P* < 0.01 comparing *Abcb1a/1b*^{-/-} to *Abcb1a/1b;Abcg2*^{-/-} mice.

1b;Abcg2^{-/-} mice compared to WT mice (Fig. 4A), and the brain-to-plasma ratios were significantly increased in both *Abcb1a/1b*^{-/-} (2.2-fold) and *Abcb1a/1b;Abcg2*^{-/-} (2.6-fold) mice compared to WT mice (Fig. 4B; Table 2). The observation that the brain-to-plasma ratio was further significantly higher in the *Abcb1a/1b;Abcg2*^{-/-} mice than in the *Abcb1a/1b*^{-/-} mice (*P* < 0.01) suggests that mAbcg2 also contributed to reducing the brain accumulation of tivozanib (Fig. 4B). Collectively, these data indicate that the brain penetration of tivozanib was limited by both mAbcb1 and mAbcg2, albeit with a substantially bigger role for mAbcb1.

In contrast to the brain, loss of both Abcb1 and Abcg2 transporters resulted in a 1.3-fold lower liver-to-plasma ratio in *Abcb1a/1b;Abcg2*^{-/-} compared to WT mice (Fig. 4B; Table 2). This result was in line with our previous 8 h pilot experiment, which showed a 1.4-fold lower liver-to-plasma ratio (Supplemental Figure 6D; Supplemental Table 1). We further analyzed the kidney and spleen concentrations (Supplemental Figure 8) of tivozanib. As in the previous 24 h and 8 h experiments, we found no substantial effect of mAbcb1 and mAbcg2 on relative tivozanib distribution to kidney and spleen after oral administration.

3.7. mOatp1a/1b transporters may have a minor role in the distribution of tivozanib to the liver

To investigate the roles of the Oatp1a/1b uptake transporters in tivozanib disposition, we also performed an 8 h oral experiment in WT and Oatp1a/1b knockout mice (*Slco1a1b*^{-/-}). No significant differences were observed in the plasma AUC over 8 h between WT and *Slco1a1b*^{-/-} mice, and the plasma concentrations remained at relatively high levels until 8 h (Supplemental Figure 5B).

For the *Slco1a1b*^{-/-} mice, we observed a significant decrease (1.2-fold) in liver-to-plasma ratio compared to WT mice (Supplemental Figure 9D; Supplemental Table 2). However, this difference was small, indicating that there could be at best a small contribution of Oatp1a/1b to the uptake of tivozanib into the liver. In contrast to the liver-to-plasma ratio, there were no significant differences in brain-, kidney- and spleen-to-plasma ratios of tivozanib, suggesting that there is no meaningful impact of mouse Oatp1a/1b transporters on tivozanib distribution to brain, kidney, and spleen (Supplemental Figure 9; Supplemental Table 2).

4. Discussion

In this study, we found that tivozanib is transported by hABCB1 and mAbcg2 *in vitro*, and that this transport can be inhibited with specific inhibitors. However, we did not observe a clear limiting effect of

mAbcb1a/1b and/or mAbcg2 on the oral availability of tivozanib in mice. Tivozanib was absorbed quickly, but the plasma concentrations stayed at high levels between 15 min and 8 h, suggesting the presence of enterohepatic circulation. The brain penetration of tivozanib was limited by the combined function of mAbcb1 and mAbcg2 (2.6-fold), and by single mAbcb1 activity as well (2.2-fold) (Figs. 3 and 4A, B). Thus, both mAbcb1 and, to a lesser extent, mAbcg2 can modestly restrict brain accumulation of tivozanib in mice. Qualitatively, this ABC transporter-drug interaction behavior at the BBB is similar to that seen for a number of other targeted anticancer drugs, including the VEGFR inhibitors sorafenib (Tang et al. 2013), sunitinib (Tang et al. 2012) and axitinib (Poller et al. 2011).

The administered dose we used in mice (1 mg/kg) was substantially higher than the recommended therapeutic dose for tivozanib (1.5 mg/d) in patients, primarily to facilitate ready detection in tissues. We indeed found C_{max} and plateau plasma levels in our mice of around 300 ng/ml, about 4–5-fold higher than therapeutic C_{max} levels in chronically treated patients (Jang and Atkins). Nonetheless, the plasma exposure was still of the same order of magnitude as used in patients. At this relatively high single dose we did not observe any acute toxicity, suggesting that tivozanib was well tolerated in mice under these conditions. Compared to other VEGFR inhibitors, the recommended therapeutic dose for tivozanib (1.5 mg/d) is far lower than for sorafenib (400 mg/d) and sunitinib (50 mg/d). The brain-to-plasma ratio in WT mice for tivozanib (~14%) was higher than that of sorafenib (~3%), lower than that of sunitinib (30%), and similar to that for axitinib (~12%) (Tang et al. 2013, Poller et al. 2011). This suggests that tivozanib has a relatively good ability to accumulate into the mouse brain. As 9% of RCC patients have brain metastases, theoretically, one could therefore consider to try and further improve the brain concentration of tivozanib by co-administration of a strong ABCB1 and ABCG2 inhibitor, such as elacridar, as was previously demonstrated in mice for sunitinib (Tang et al. 2012). This might help to enhance drug exposure for tumors that are positioned in part or in whole behind the BBB, and thus possibly improve therapeutic efficacy. However, the effect of Abcb1 and Abcg2 on brain penetration of tivozanib was relatively modest. If this would also apply to the human brain, this might perhaps mean that the gain from such a co-administration approach would be relatively limited.

The plasma pharmacokinetic profile of tivozanib showed quick absorption, and plasma concentration–time curves from patients and mice both show secondary peaks, indicating that tivozanib may undergo enterohepatic recirculation. This would likely be a contributing factor in the observed late t_{max}. In our 24 h experiment, the average half-life (t_{1/2}) was 335 min (188–588 min), i.e. 3.1–9.8 h (average 5.6 h) in

mice. This long half-life and high variability between mice is in line with the clinical experiment of Eskens *et al.*, which revealed a $t_{1/2}$ of 4.7 days (112 h), range 31 to 233 h in patients (Eskens *et al.* 2011). Compared to other VEGFR inhibitors (sunitinib ($t_{1/2}$, 41–86 h) (Faivre *et al.* 2006), sorafenib ($t_{1/2}$, 20–36 h) (Moore *et al.* 2005), and axitinib ($t_{1/2}$, 2–5 h) (Rugo *et al.* 2005)) in patients, tivozanib's extended half-life could enhance the exposure of tumors to tivozanib, which has positive clinical implications. The plateau-like pharmacokinetic profile of tivozanib may also allow for more consistent therapeutic levels without large fluctuations in concentration between daily doses and allows the current once-daily dosing schedule.

Somewhat unexpectedly, after oral administration, the *Abcg2*^{-/-} and *Abcb1a/1b;Abcg2*^{-/-} mice demonstrated modestly reduced liver-to-plasma ratios of tivozanib at 8 h (Fig. 4D, Supplemental Figure 6D). This may perhaps reflect a partially reduced *Abcg2*-mediated biliary excretion from the hepatocytes into bile. As a result, the reduced intrahepatic biliary tivozanib concentration may have slightly reduced overall liver-to-plasma ratios of tivozanib in *Abcg2*^{-/-} and *Abcb1a/1b;Abcg2*^{-/-} mice (gall bladders were always removed from the liver before homogenization), assuming that the intrahepatic bile contributes importantly to overall hepatic tivozanib concentration. However, the direct functions of *Abcg2* and *Abcb1* in this putative process are limited, considering the small difference between the WT and *Abcb1a/1b;Abcg2*^{-/-} mice (~0.8-fold).

Looking at the collective *in vitro* and *in vivo* data, it is theoretically possible that ABCB1 and ABCG2 expression in RCC cells might directly contribute to some level of resistance to tivozanib therapy. However, its absolute contribution, if any, is likely to be small. Reustle *et al.* found decreased ABCB1 mRNA expression, but increased ABCG2 mRNA expression in clear cell RCC tissue compared to non-tumor tissue (Reustle *et al.* 2018), which might perhaps also affect tivozanib resistance.

Very little literature is available on the possible interaction of tivozanib with OATPs. Our experiments in *Slco1a/1b*^{-/-} mice suggest there might perhaps be a modest uptake function of *mOatp1a/1b* transporters in tivozanib liver accumulation, but the differences in liver-to-plasma ratio between WT and *Slco1a/1b*^{-/-} mice were small (1.2-fold), and plasma levels were not affected. Any broader *in vivo* pharmacokinetic impact of variable OATP activity in patients is therefore likely to be small.

We found no significant differences in the plasma AUCs and tissue-to-plasma ratios in WT, *Cyp3a*^{-/-} and *Cyp3aXAV* mice (Fig. 2B; Table 1). The data suggest that *mCyp3a* or *hCYP3A4* in themselves do not significantly affect tivozanib detoxification. According to the EMA report, CYP1A1 and CYP3A4 can metabolize tivozanib *in vitro* (EMA 2017), but the *in vivo* impact of CYP3A appears to be negligible. This is in line with the absence of a clear effect of CYP3A inhibition on tivozanib plasma levels in patients (Cotureau *et al.* 2015). The modest reduction in late clearance in both CYP3A-modified strains we observed (Supplemental Fig. 2B) suggests that the absence of mouse *Cyp3a* (but not the presence of human CYP3A4) alters some other tivozanib-eliminating process. We have earlier documented some compensatory changes in *Cyp3a* knockout mice, primarily upregulation of *Cyp2c* enzymes (van Waterschoot *et al.* 2008). However, this could not explain decreased clearance of tivozanib, so some other unidentified detoxification system may have been (modestly) altered.

5. Conclusion

Our data indicate that both *Abcb1a/1b* and *Abcg2* can modestly restrict the net accumulation of tivozanib in the brain, but not its oral availability. If also true in humans, the observed modest effect of ABC transporters on brain accumulation of tivozanib suggests that this drug, in contrast to most other TKIs, will only be modestly limited by the ABC transporters in its therapeutic efficacy against malignant lesions situated in part or in whole behind the BBB. We further found that *mOatp1a/1b* had at best a very modest uptake function for tivozanib

into liver, without affecting overall plasma kinetics. Finally, both *mCyp3a* and human CYP3A4 appear to have little if any direct impact on the *in vivo* oral availability and tissue distribution of tivozanib. Collectively, our data suggest that OATP- and CYP3A-related drug-drug interactions or genetic polymorphisms are probably of minor concern for the clinical application of tivozanib.

Declaration of Competing Interest

The authors declare that they have no known competing financial interests or personal relationships that could have appeared to influence the work reported in this paper.

Acknowledgements

This work was supported in part by a fellowship from the China Scholarship Council (to C.G., number 201506240145) and internal funds from the Netherlands Cancer Institute.

Appendix A. Supplementary data

Supplementary data to this article can be found online at <https://doi.org/10.1016/j.ijpharm.2020.119277>.

References

- AVEO Oncology, 2017. AVEO Oncology announces FOTIVDA® (tivozanib) approved in the European Union for the Treatment of advanced renal cell carcinoma.
- Bianchi, M., Sun, M., Jeldres, C., Shariat, S., Trinh, Q.-D., Briganti, A., Tian, Z., Schmitges, J., Graefen, M., Perrotte, P., 2011. Distribution of metastatic sites in renal cell carcinoma: a population-based analysis. *Ann. Oncol.* 23, 973–980.
- Borst, P., Elferink, R.O., 2002. Mammalian ABC transporters in health and disease. *Annu. Rev. Biochem.* 71, 537–592.
- Bruin, M.A.C., Rosing, H., Lucas, L., Wang, J., Huitema, A., Schinkel, A., Beijnen, J., 2019. Development and validation of an LC-MS/MS method with a broad linear dynamic range for the quantification of tivozanib in human and mouse plasma, mouse tissue homogenates, and culture medium. *J. Chromatogr. B* 1125, 121723.
- Cheng, X., Klaassen, C.D., 2009. Tissue distribution, ontogeny, and hormonal regulation of xenobiotic transporters in mouse kidneys. *Drug Metab. Dispos.* 37, 2178–2185.
- Cheng, X., Maher, J.M., Chen, C., Klaassen, C.D., 2005. Tissue distribution and ontogeny of mouse organic anion transporting polypeptides (Oatps). *Drug Metab. Dispos.* 33, 1062–1073.
- Cotureau, M.M., Siebers, N.M., Miller, J., Strahs, A.L., Slichenmyer, W., 2015. Effects of ketoconazole or rifampin on the pharmacokinetics of tivozanib hydrochloride, a vascular endothelial growth factor receptor tyrosine kinase inhibitor. *Clin. Pharmacol. Drug Dev.* 4, 137–142.
- Durmus, S., Sparidans, R.W., Wagenaar, E., Beijnen, J.H., Schinkel, A.H., 2012. Oral availability and brain penetration of the B-RAFV600E inhibitor vemurafenib can be enhanced by the P-GLYCOPROTEIN (ABCB1) and breast cancer resistance protein (ABCG2) inhibitor elacridar. *Mol. Pharm.* 9, 3236–3245.
- EMA, 2017. Committee for Medicinal Products for Human Use (CHMP), European Medicines Agency (EMA), Assessment Report: Fotivda (Tivozanib).
- Eskens, F.A., de Jonge, M.J., Bhargava, P., Ise, T., Cotureau, M.M., Esteves, B., Hayashi, K., Burger, H., Thomeer, M., van Doorn, L., 2011. Biologic and clinical activity of tivozanib (AV-951, KR-951), a selective inhibitor of VEGF receptor-1, -2, and -3 tyrosine kinases, in a 4-week-on, 2-week-off schedule in patients with advanced solid tumors. *Clin. Cancer Res.* 17, 7156–7163.
- Faivre, S., Delbaldo, C., Vera, K., Robert, C., Lozahic, S., Lassau, N., Bello, C., Deprimo, S., Brega, N., Massimini, G., 2006. Safety, pharmacokinetic, and antitumor activity of SU11248, a novel oral multitarget tyrosine kinase inhibitor, in patients with cancer. *J. Clin. Oncol.* 24, 25–35.
- Giacomini, K.M., Huang, S.-M., Tweedie, D.J., Benet, L.Z., Brouwer, K.L., Chu, X., Dahlin, A., Evers, R., Fischer, V., Hillgren, K.M., 2010. Membrane transporters in drug development. *Nat. Rev. Drug Discovery* 9, 215.
- Gong, J., Maia, M.C., Dizman, N., Govindarajan, A., Pal, S.K., 2016. Metastasis in renal cell carcinoma: Biology and implications for therapy. *Asian journal of urology* 3, 286–292.
- Guengerich, F.P. 1995. Human cytochrome P450 enzymes. In *Cytochrome P450*, 473–535. Springer.
- Jang, S., Atkins, M., 2014. Treatment of BRAF-mutant melanoma: the role of vemurafenib and other therapies. *Clin. Pharmacol. Ther.* 95, 24–31.
- Jonker, J.W., Buitelaar, M., Wagenaar, E., Van Der Valk, M.A., Scheffer, G.L., Schepers, R.J., Plösch, T., Kuipers, F., Elferink, R.P.O., Rosing, H., 2002. The breast cancer resistance protein protects against a major chlorophyll-derived dietary phototoxin and protoporphyria. *Proc. Natl. Acad. Sci.* 99, 15649–15654.
- Jonker, J.W., Freeman, J., Bolscher, E., Musters, S., Alvi, A.J., Tittley, I., Schinkel, A.H., Dale, T.C., 2005. Contribution of the ABC transporters Bcrp1 and Mdr1a/1b to the

- side population phenotype in mammary gland and bone marrow of mice. *Stem Cells* 23, 1059–1065.
- Moore, M., Hirte, H., Siu, L., Oza, A., Hotte, S., Petrenciuc, O., Cihon, F., Lathia, C., Schwartz, B., 2005. Phase I study to determine the safety and pharmacokinetics of the novel Raf kinase and VEGFR inhibitor BAY 43–9006, administered for 28 days on/7 days off in patients with advanced, refractory solid tumors. *Ann. Oncol.* 16, 1688–1694.
- Motzer, R.J., Nosov, D., Eisen, T., Bondarenko, I., Lesovoy, V., Lipatov, O., Tomczak, P., Lyulko, O., Alyasova, A., Harza, M., 2013. Tivozanib versus sorafenib as initial targeted therapy for patients with metastatic renal cell carcinoma: results from a phase III trial. *J. Clin. Oncol.* 31, 3791.
- Poller, B., Iusuf, D., Sparidans, R.W., Wagenaar, E., Beijnen, J.H., Schinkel, A.H., 2011. Differential impact of P-glycoprotein (ABCB1) and breast cancer resistance protein (ABCG2) on axitinib brain accumulation and oral plasma pharmacokinetics. *Drug Metab. Dispos.* 39, 729–735.
- Reustle, A., Fisel, P., Renner, O., Büttner, F., Winter, S., Rausch, S., Kruck, S., Nies, A.T., Hennenlotter, J., Scharpf, M., 2018. Characterization of the breast cancer resistance protein (BCRP/ABCG2) in clear cell renal cell carcinoma. *Int. J. Cancer* 143, 3181–3193.
- Rugo, H.S., Herbst, R.S., Liu, G., Park, J.W., Kies, M.S., Steinfeldt, H.M., Pithavala, Y.K., Reich, S.D., Freddo, J.L., Wilding, G., 2005. Phase I trial of the oral antiangiogenesis agent AG-013736 in patients with advanced solid tumors: pharmacokinetic and clinical results. *J. Clin. Oncol.* 23, 5474–5483.
- Schinkel, A.H., Jonker, J.W., 2003. Mammalian drug efflux transporters of the ATP binding cassette (ABC) family: an overview. *Adv. Drug Deliv. Rev.* 55, 3–29.
- Schinkel, A.H., Mayer, U., Wagenaar, E., Mol, C.A., Van Deemter, L., Smit, J.J., Van Der Valk, M.A., Voordouw, A.C., Spits, H., Van Tellingen, O., 1997. Normal viability and altered pharmacokinetics in mice lacking mdr1-type (drug-transporting) P-glycoproteins. *Proc. Natl. Acad. Sci.* 94, 4028–4033.
- Tang, S.C., de Vries, N., Sparidans, R.W., Wagenaar, E., Beijnen, J.H., Schinkel, A.H., 2013. Impact of P-glycoprotein (ABCB1) and breast cancer resistance protein (ABCG2) gene dosage on plasma pharmacokinetics and brain accumulation of dasatinib, sorafenib, and sunitinib. *J. Pharmacol. Exp. Ther.* 346, 486–494.
- Tang, S.C., Lagas, J.S., Lankheet, N.A., Poller, B., Hillebrand, M.J., Rosing, H., Beijnen, J.H., Schinkel, A.H., 2012. Brain accumulation of sunitinib is restricted by P-glycoprotein (ABCB1) and breast cancer resistance protein (ABCG2) and can be enhanced by oral elacridar and sunitinib coadministration. *Int. J. Cancer* 130, 223–233.
- van de Steeg, E., Wagenaar, E., van der Kruijssen, C.M., Burggraaff, J.E., de Waart, D.R., Elferink, R.P.O., Kenworthy, K.E., Schinkel, A.H., 2010. Organic anion transporting polypeptide 1a/1b-knockout mice provide insights into hepatic handling of bilirubin, bile acids, and drugs. *J. Clin. Investig.* 120, 2942–2952.
- van Herwaarden, A.E., Wagenaar, E., van der Kruijssen, C.M., van Waterschoot, R.A., Smit, J.W., Song, J.-Y., van der Valk, M.A., van Tellingen, O., van der Hoorn, J.W., Rosing, H., 2007. Knockout of cytochrome P450 3A yields new mouse models for understanding xenobiotic metabolism. *J. Clin. Investig.* 117, 3583–3592.
- van Hoppe, S., Sparidans, R.W., Wagenaar, E., Beijnen, J.H., Schinkel, A.H., 2017. Breast cancer resistance protein (BCRP/ABCG2) and P-glycoprotein (P-gp/ABCB1) transport afatinib and restrict its oral availability and brain accumulation. *Pharmacol. Res.* 120, 43–50.
- van Waterschoot, R.A., Rooswinkel, R.W., Wagenaar, E., van der Kruijssen, C.M., van Herwaarden, A.E., Schinkel, A.H., 2009. Intestinal cytochrome P450 3A plays an important role in the regulation of detoxifying systems in the liver. *FASEB J.* 23, 224–231.
- van Waterschoot, R.A., van Herwaarden, A.E., Lagas, J.S., Sparidans, R.W., Wagenaar, E., van der Kruijssen, C.M., Goldstein, J.A., Zeldin, D.C., Beijnen, J.H., Schinkel, A.H., 2008. Midazolam metabolism in cytochrome P450 3A knockout mice can be attributed to up-regulated CYP2C enzymes. *Mol. Pharmacol.* 73, 1029–1036.
- Vlaming, M.L., Lagas, J.S., Schinkel, A.H., 2009. Physiological and pharmacological roles of ABCG2 (BCRP): recent findings in Abcg2 knockout mice. *Adv. Drug Deliv. Rev.* 61, 14–25.
- Wang, J., Gan, C., Retmana, I.A., Sparidans, R.W., Li, W., Lebre, M.C., Beijnen, J.H., Schinkel, A.H., 2019. P-glycoprotein (MDR1/ABCB1) and Breast Cancer Resistance Protein (BCRP/ABCG2) limit brain accumulation of the FLT3 inhibitor quizartinib in mice. *Int. J. Pharm.* 556, 172–180.
- Wang, J., Gan, C., Sparidans, R.W., Wagenaar, E., van Hoppe, S., Beijnen, J.H., Schinkel, A.H., 2018. P-glycoprotein (MDR1/ABCB1) and breast cancer resistance protein (BCRP/ABCG2) affect brain accumulation and intestinal disposition of encorafenib in mice. *Pharmacol. Res.* 129, 414–423.
- Yang, D., Kathawala, R.J., Chufan, E.E., Patel, A., Ambudkar, S.V., Chen, Z.-S., Chen, X., 2014. Tivozanib reverses multidrug resistance mediated by ABCB1 (P-glycoprotein) and ABCG2 (BCRP). *Future Oncol.* 10, 1827–1841.
- Zanger, U.M., Schwab, M., 2013. Cytochrome P450 enzymes in drug metabolism: regulation of gene expression, enzyme activities, and impact of genetic variation. *Pharmacol. Ther.* 138, 103–141.
- Zhang, Y., Huo, M., Zhou, J., Xie, S., 2010. PKSolver: An add-in program for pharmacokinetic and pharmacodynamic data analysis in Microsoft Excel. *Comput. Methods Programs Biomed.* 99, 306–314.